

PAPER • OPEN ACCESS

Axial absorbed dose distributions during abdominal computed tomography acquisitions: Measurement and the Monte Carlo simulation study

To cite this article: K Matsubara *et al* 2019 *J. Phys.: Conf. Ser.* **1248** 012020

View the [article online](#) for updates and enhancements.



IOP | ebooks™

Bringing together innovative digital publishing with leading authors from the global scientific community.

Start exploring the collection—download the first chapter of every title for free.

Axial absorbed dose distributions during abdominal computed tomography acquisitions: Measurement and the Monte Carlo simulation study

K Matsubara¹, H Nagata², R Okubo³, Y Ogawa³, T Chusin³ and A Hirosawa³

¹ Department of Quantum Medical Technology, Faculty of Health Sciences, Institute of Medical, Pharmaceutical and Health Sciences, Kanazawa University, Kanazawa, Japan

² Section of Radiological Technology, Department of Medical Technology, Kanazawa Medical University Hospital, Uchinada, Japan

³ Department of Quantum Medical Technology, Division of Health Sciences, Graduate School of Medical Science, Kanazawa University, Kanazawa, Japan

E-mail: matsuk@mhs.mp.kanazawa-u.ac.jp

Abstract. We aimed to validate Monte Carlo (MC) simulation models against measurements and evaluate the effect of object size on axial absorbed dose distributions during abdominal computed tomography (CT) acquisitions based on MC simulations. A medium-sized abdominal phantom, with holes to insert a pencil ionization chamber, was acquired using a 192-slice dual-source CT scanner at a tube voltage of 120 kVp and a displayed volume CT dose index of 5.0 mGy. Absorbed doses were measured using the pencil ionization chamber and an electrometer, and normalized absorbed doses to center were calculated for all measurement locations. The Particle and Heavy Ion Transport code System version 3.02 was used to simulate normalized absorbed doses of 19 locations through small-, medium-, and large-sized abdominal phantom models with a tube voltage of 120 kVp. In the measurement and MC simulation, the normalized absorbed dose to center in the medium-sized abdominal phantom was 1.48 ± 0.28 and 1.62 ± 0.35 , respectively. Higher normalized doses were observed at peripheral regions when the phantom size was larger.

1. Introduction

In modern CT scanners, the X-ray tube voltage ranges from 70 to 150 kVp, but a tube voltage of 120 kVp is typically used in the majority of CT protocols because it yields sufficient X-ray energy to penetrate most parts of the anatomy [1]. However, the appropriate tube voltage depends on the size of the patient because photons need more energy to penetrate a larger patient and less energy to penetrate a smaller patient [2].

Monte Carlo (MC) simulations have been widely adopted to accurately and reliably estimate patient doses from CT examinations [3-5]. To obtain accurate estimates of patient doses, MC simulation models must be validated against measurements with a simple phantom in order to compare the simulated and measured values.

We aimed to validate MC simulation models against measurements using an abdominal phantom and evaluate the effect of object size on axial absorbed dose distributions during abdominal CT acquisitions based on MC simulations.



2. Materials and Methods

2.1. Measurement

2.1.1. CT scanner. A 192-slice dual-source CT scanner SOMATOM Force (Siemens Healthineers, Erlangen, Germany) was used to obtain axial absorbed dose distributions. Only one pair of X-ray tubes and detectors was used in this study.

2.1.2. Abdominal phantom. A medium-sized abdominal phantom (007TE-07; CIRS, Norfolk, VA, USA), which has five through-holes with an inside diameter of 1.30 cm, was used to accommodate a CT ionization chamber and tissue-equivalent rods to plug the holes. In addition to these five holes, we drilled eight through holes of the same diameter in the right side of the phantom (Figure 1) to obtain detailed axial absorbed dose distribution.

When axial absorbed dose distribution was obtained in the left side of the phantom, the left/right position of the phantom was turned. Hence, absorbed doses of 19 locations were acquired to assess the axial absorbed dose distribution.

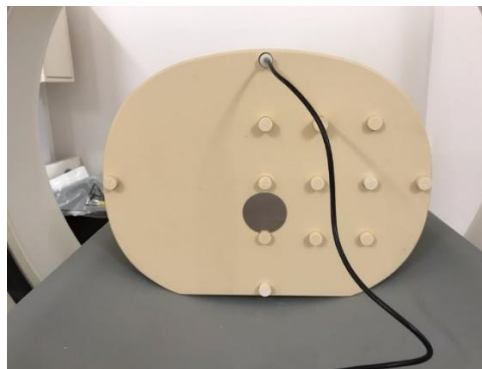


Figure 1. A medium-sized abdominal phantom with longitudinal diameter of 25.0 cm, transverse diameter of 32.5 cm, and thickness of 15.0 cm. The body of the phantom was made by Plastic Water LR, and the phantom included a vertebral bone-equivalent rod.

2.1.3. Measurement of absorbed doses. Using laser lights, the abdominal phantom was positioned at the isocenter of the CT gantry on the CT table. A pencil ionization chamber with an active length of 100 mm (20X6-3CT; Radcal, Monrovia, CA, USA) was connected to an electrometer (2023C; Radcal) and used to measure the air kerma, which was almost equal to the absorbed dose in air in the diagnostic energy range, of 19 locations.

The pencil ionization chamber was inserted into one of the holes, the other holes were plugged with rods, and the phantom was imaged by a single axial scan at a tube voltage of 120 kVp, tube current of 75 mA, collimation of 192×0.6 mm, and tube rotation time of 1.0 sec/rot (displayed volume CT dose index [CTDI_{vol}] of 4.97 mGy).

Each location was measured five times to reduce random error, and the average absorbed dose for each location was calculated. The normalized absorbed dose to center was calculated for all measurement locations.

2.2. MC Simulation

2.2.1. MC simulation code. The Particle and Heavy Ion Transport code System, version 3.02, [6] was used as the MC simulation code. All simulations were performed with a low-energy cutoff of 1 keV for photons.

2.2.2. Phantom model. Small-, medium-, and large-sized abdominal phantom models were built (Figure 2) according to a data sheet of 007TE phantoms (CIRS). The circles shown in Figure 2 represent the locations with a longitudinal length of 10 cm to be tallied. We used Plastic Water material, and the phantom bodies had a density of 1.029 g/cm^3 ; their mass fraction compositions were 7.4% hydrogen, 2.26% boron, 46.7% carbon, 1.56% nitrogen, 33.52% oxygen, 6.88% magnesium, 1.4% aluminum, and 0.24% chlorine [7].

We used mass fraction compositions of B-100 Bone-Equivalent Plastic because those of the vertebral bone-equivalent rod were not provided by the vendor: 6.5473% hydrogen, 53.6942% carbon, 2.1500% nitrogen, 3.2084% oxygen, 16.7415% fluorine, and 17.6585% calcium [8].

The phantom models were positioned on a model of the CT table, which was built based on the CT image of the CT table. The case and the interior of the table were modeled as carbon fiber (density 1.6 g/cm^3) and Styrofoam (density 0.015 g/cm^3), respectively.

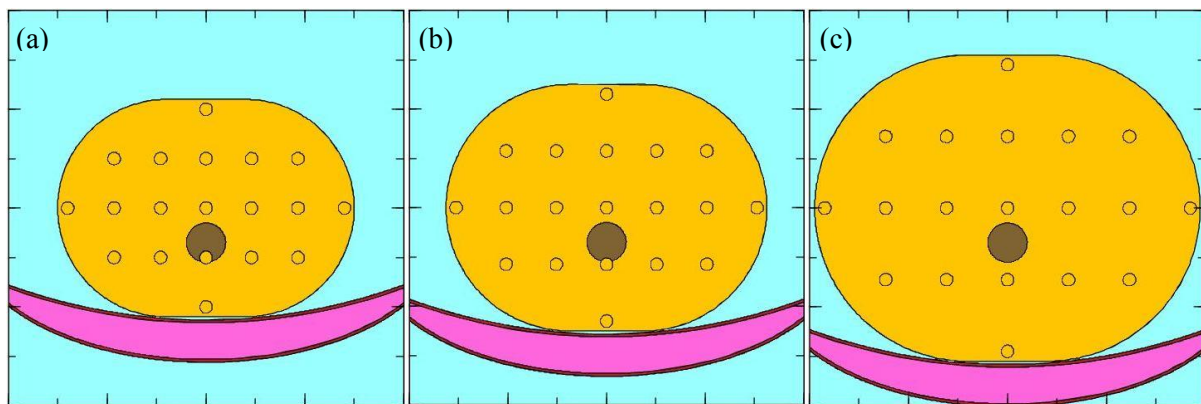


Figure 2. Different-sized abdominal phantom models with a thickness of 15.0 cm: (a) small-sized abdominal phantom model with a longitudinal diameter of 22.0 cm and a transverse diameter of 30.0 cm, (b) medium-sized abdominal phantom model with a longitudinal diameter of 25.0 cm and a transverse diameter of 32.5 cm, (c) large-sized abdominal phantom model with a longitudinal diameter of 31.0 cm and a transverse diameter of 38.9 cm.

2.2.3. Source model. We used X-Tucker-31 software to calculate the X-ray energy spectrum [9]. This software generates X-ray energy spectra from a tungsten target based on generator type, peak tube voltage, and filtration using Tucker's formula [10]. In the present study, the X-ray energy spectrum was calculated using the software for a tungsten target at a tube voltage of 120 kVp, target angle of 8° , and aluminum half-value layer of 8.03 mm. The aluminum half-value layer was obtained previously using the non-rotating method with the CT scanner in service mode [11].

Source to isocenter distance was 59.5 cm, and the default cone-shaped X-ray beam was collimated to a longitudinal width of 5.76 cm. The fan angle of the X-ray beam was 50° .

Aluminum was chosen as the basic material of the bowtie filter, and its shape was estimated using the characterization of bowtie relative attenuation (COBRA) method, which characterizes the CT scanner's bowtie filter using a real-time exposure meter [12,13]. A CT Dose Profiler (RTI, Mölnådal, Sweden) was used as a real-time dosimeter.

2.2.4. MC simulation condition. During calculation, 10^7 photons/projection were irradiated from 24 projections (per 360° rotation) so that the relative errors (coefficients of variance) of the tallied results were $<1\%$. By using [T-Heat] function, deposit energy estimated using the kerma approximation, which is almost equal to the absorbed dose in the diagnostic energy range, in 19 locations (shown by the circles in Figure 2) was tallied in units of Gy/source. After calculating 24 projections, the tallied results were summed by setting icntl = 13 (sumtally function). The calculation was performed three times to reduce

random error, and the average absorbed dose was calculated for each tallied location. Moreover, normalized absorbed dose to center was calculated for each tallied location.

2.3. Dose distribution map

Absorbed dose distribution maps were drawn using OriginPro 2019 (OriginLab, Northampton, MA, USA) graph drawing software based on the results of the normalized absorbed dose to center for 19 locations. In the software, Delaunay Triangulation was used to compute and draw the contour lines of the absorbed dose distribution maps.

3. Results

3.1. Validation of MC simulations

Axial dose distributions acquired from the measurement and simulation results are shown in Figure 3. The normalized absorbed dose to center in the medium-sized abdominal phantom was 1.48 ± 0.28 in the measurement and 1.62 ± 0.35 in the MC simulations. The average relative difference of the normalized absorbed doses between the measurement and MC simulations was 8.87%.

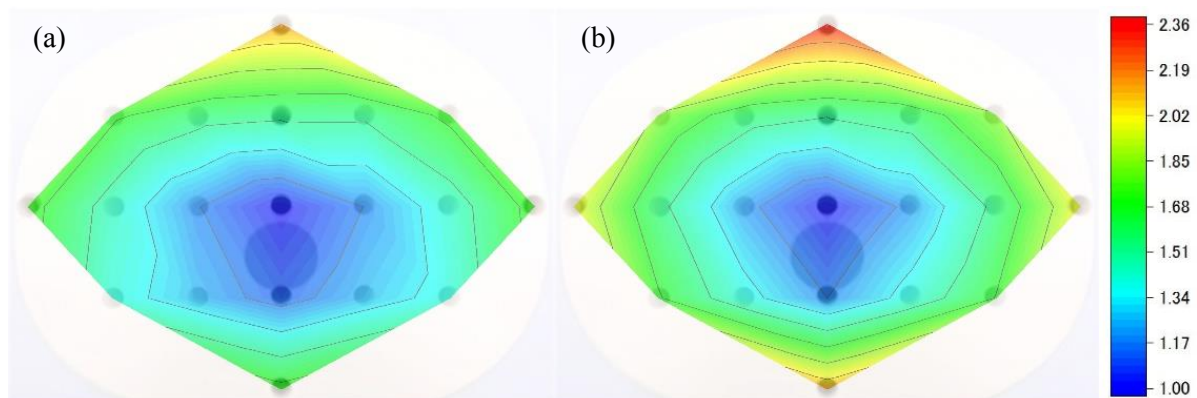


Figure 3. Axial dose distributions in medium-sized abdominal phantom: (a) measurement result, (b) MC simulation result

3.2. Comparison of MC simulation results among different-sized phantom models

Axial dose distributions among different-sized phantom models obtained from MC simulations are shown in Figure 4. The normalized absorbed doses to center were 1.47 ± 0.28 , 1.62 ± 0.35 , and 2.01 ± 0.59 in the small-, medium-, and large-sized phantom models, respectively.

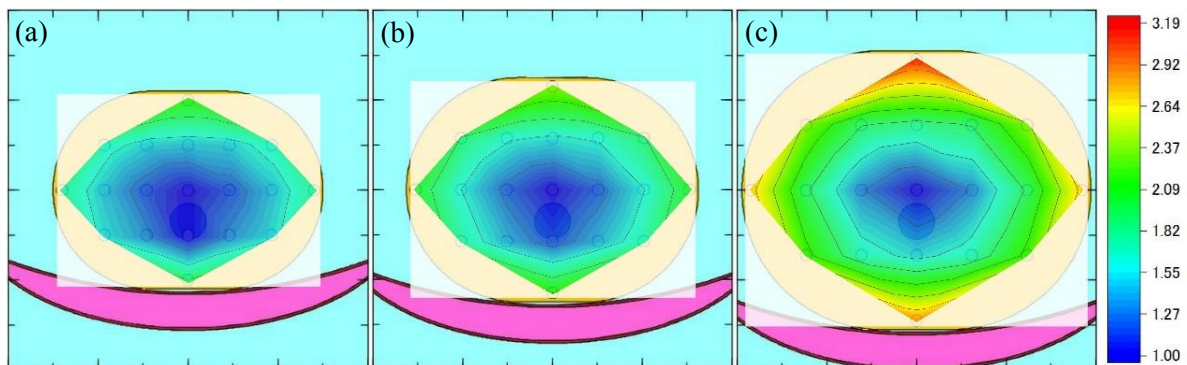


Figure 4. Axial dose distributions among different-sized phantom models obtained from MC simulations: (a) small-sized phantom model, (b) medium-sized phantom model, (c) large-sized phantom model

4. Discussion

We calculated axial absorbed dose distributions during abdominal CT acquisitions based on measurement and MC simulations. The normalized absorbed doses to center in the medium-sized abdominal phantom were 1.48 ± 0.28 and 1.62 ± 0.35 in the measurement and MC simulations, respectively. According to the MC simulation results among the different-sized phantom models, peripheral regions had higher normalized doses when the phantom size was larger.

The average relative difference of the normalized absorbed doses between the measurement and MC simulations was 8.87%. We think the difference was mostly due to the accuracy of the MC simulation model.

Although determining the X-ray energy spectrum is an important task when performing dose calculation with MC simulations, measuring X-ray energy spectra directly from a CT scanner is impossible due to the high photon flux produced by the X-ray tubes. Instead, we used software to simulate X-ray energy spectra using a semi-empirical model based on Tucker's formula [10]. The software uses half-value layer to estimate total filtration; however, it is represented by thickness in aluminum-equivalent units, and the filtrations were not the actual thicknesses and materials of the filter inside the CT scanner.

We used the COBRA method [12,13] to estimate the bowtie filter thicknesses along the fan angle. The COBRA method was a fast and accurate method for characterizing bowtie filters in a clinical CT scanner [13]. In the present study, we chose aluminum as the material for the bowtie filter, but the composition of the bowtie filter is not available in user manuals or CT technical specifications because it is not disclosed by CT vendors. We think the estimation of bowtie filter attenuation will be more accurate when the composition of the bowtie filter is revealed.

The commercially available medium-sized abdominal phantom was used for measurement, and three different-sized phantom models were built by referring to the data sheet of the medium-sized abdominal phantom. The body of the phantom was made by Plastic Water LR, but the phantom bodies used in our MC simulations were made by Plastic Water because the phantom vendor did not disclose the composition of Plastic Water LR. The shape of the abdominal phantom was a bit different from those of the phantom models. The shape and materials of the CT table were also different from those of the CT table model in the MC simulations.

A previous study showed that the relative CTDI difference between the measurement and MC simulations was <10%, which was less than our results [14]. However, the authors used standard polymethyl methacrylate head and body phantoms, which had a simple structure and their models were fairly easy to build.

A method of optimizing patient dose is to adjust the X-ray tube current using a weight- or size-based protocol. Automatic tube current modulation techniques can adjust tube current to maintain constant image quality at the lowest dose [15]. Our results show that higher normalized doses occurred at peripheral regions using the same tube voltage (120 kVp) when the phantom size was larger. Although reducing the tube voltage is effective for increasing image contrast of iodine-enhanced CT, tube voltage should be optimized according to the size of the patient to obtain more uniform axial dose distribution. Recently introduced automatic tube voltage selection techniques, such as CARE kV (Siemens Healthineers) and kV Assist (GE Healthcare, Chicago, IL, USA), enable the CT scanner to select the optimal tube voltage for the particular patient size and selected clinical requirement [16]. The scanner can suggest the lowest tube voltage and tube current combination for obtaining the lowest patient dose for the defined image quality, but it is not clear whether the lowest tube voltage provides the most uniform axial dose distribution. The relationships of tube voltage, axial absorbed dose distribution, and image quality are complicated, and thus should be further investigated.

In this study, we evaluated the effect of object size on axial absorbed dose distributions using a tube voltage of only 120 kVp. Axial absorbed dose distributions obtained using other tube voltages will be useful for optimizing tube voltage according to patient size. There were only one CT scanner and one source model involved in this study. Therefore, similar studies should be performed using different CT scanners and source models.

5. Conclusion

We investigated the effect of object size on axial absorbed dose distributions during abdominal CT acquisitions based on MC simulations validated against measurements. The average relative difference of the normalized doses between the measurement and MC simulations was 8.87%. MC simulations demonstrated that normalized doses were higher at peripheral regions when larger phantoms were imaged.

References

- [1] Mahesh M 2009 *MDCT Physics: The Basics: Technology, Image Quality and Radiation Dose* (Philadelphia, PA: Lippincott Williams & Wilkins)
- [2] Nagayama Y, Oda S, Nakaura T, Tsuji A, Urata J, Furusawa M, Utsunomiya D, Funama Y, Kidoh M and Yamashita Y 2018 *Radiographics* **38** 1421–40
- [3] DeMarco JJ, Cagnon CH, Cody DD, Stevens DM, McCollough CH, O'Daniel J and McNitt-Gray MF 2005 *Phys. Med. Biol.* **50** 3989–4004
- [4] Liu H, Gu J, Caracappa PF and Xu XG 2010 *Phys. Med. Biol.* **55** 1441–51
- [5] Bostani M, McMillan K, DeMarco JJ, Cagnon CH and McNitt-Gray MF 2014 *Med. Phys.* **41** 112101
- [6] Sato T, *et al.* 2018 *J. Nucl. Sci. Technol.* **55** 684–90
- [7] Ramaseshan R, Kohli K, Cao F and Heaton R 2008 *J. App. Clin. Med. Phys.* **9** 98–111
- [8] Hubbell JH and Seltzer SM 1995 *Tables of X-Ray Mass Attenuation Coefficients and Mass Energy-Absorption Coefficients 1 keV to 20 MeV for Elements Z = 1 to 92 and 48 Additional Substances of Dosimetric Interest* (Gaithersburg, MD: National Institute of Standards and Technology)
- [9] <http://hidekikato1952.wixsite.com/radiotechnology/free-software>
- [10] Tucker DM, Barnes GT and Chakraborty DP 1991 *Med. Phys.* **18** 211–8
- [11] Matsubara K, Ichikawa K, Murasaki Y, Hirosawa A and Koshida K 2014 *J. Appl. Clin. Med. Phys.* **15** 309–16
- [12] Boone JM 2009 *Med. Phys.* **37** 40–8
- [13] McKenney SE, Nosratieh A, Gelskey D, Yang K, Huang SY, Chen L and Boone JM 2011 *Med. Phys.* **38** 1406–15
- [14] Mendes M, Costa F, Figueira C, Madeira P, Teles P and Vaz P 2015 *Radiat. Prot. Dosimetry* **165** 175–81
- [15] Kalra MK, Maher MM, Toth TL, Schmidt B, Westerman BL, Morgan HT and Saini S 2004 *Radiology* **233** 649–57
- [16] Lira D, Padole A, Kalra MK and Singh S 2015 *AJR. Am. J. Roentgenol.* **204** W4–10

Acknowledgement

This work was supported by JSPS KAKENHI Grant Number 18K07746.